High Gradient Workshop 2007
Presented 5-24-07

Formation of Taylor Cones on a Molten Metal Surface Followed by Ion Injection Into the Vacuum

Perry Wilson
SLAC

Outline

Formation of individual craters

Crater clustering

Surface Melting

Taylor cones

Ion injection

The first three topics above are a short summary of work presented at AAC06 (Lake Geneva, Wisconsin, July 2006), and slightly extended in SLAC–PUB–12354. The last two items are mostly new work.

Formation of Individual Craters

During processing, the sharpest field emission features burn off, leaving behind a single crater for both dc and rf fields.

The crater is a sign that there was a “plasma spot” in the region of the initial field emission feature.

There are at least two mechanisms for the formation of plasma spots.

The first mechanism, due to Jim Norem and his colleagues, involves the mechanical fracture of the tip of a field emission feature as the result of the tremendous E^2 force acting on it.

The second mechanism assumes that the tip of the field emission feature is melted by ion bombardment from ionized residual gas in the tip region.

Both mechanisms are probably at work on a typical accelerator structure surface.

That the tip region is liquid in some cases is verified by some work by Jens Knobloch (Dissertation, Cornell University, August 1997, p.123) on field emitters on a superconducting niobium surface.

The figure below from Knobloch's dissertation shows a plot of the total emitter current vs. current density for field emission sites that have been processed off at high electric fields. Sometimes a "starburst" is found afterward (black circles). Starbursts are evidence that a plasma was present at the site. The emitter area is shown by the diagonal lines. Note that starbursts seem to form in the area range between 10^{-16} and 10^{-15}m^2. The pulling force on a roughly hemispherical liquid tip of radius r is $(1/4)\varepsilon_0 E^2$ times a tip area of about $2\pi r^2$. The restraining force due to a surface tension T acting at the periphery of the tip gives a force of $2\pi r(2T)$. Equating these two results, assuming a liquid in hydrostatic equilibrium, gives for a field of 7 GeV/m an area of 4 x 10^{-15} m^2 and a tip radius of about 30μm. However, there is an unknown factor due to the shape of the liquid tip just before it explodes. If the radius is reduced further, the E^2 force then becomes dominant and the tip elongates and necks in. This can bring the tip emitting area and radius to the observed values.

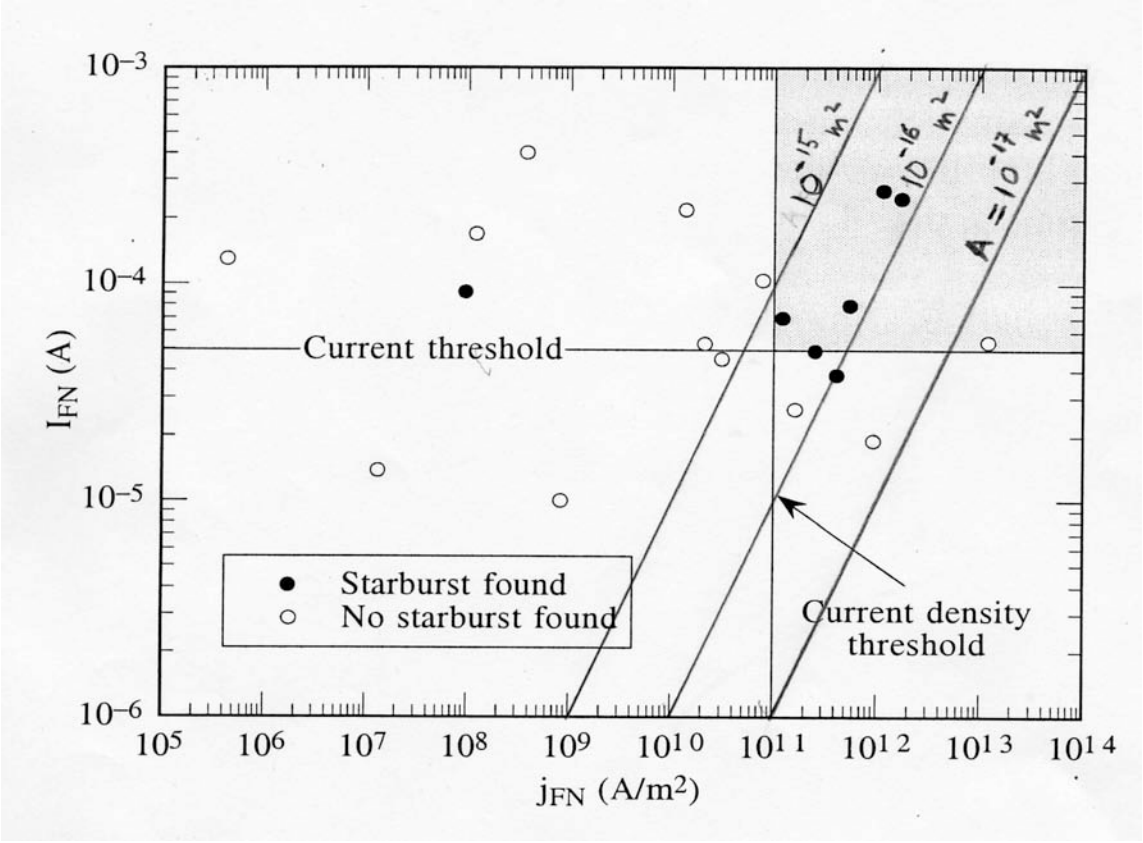

Crater Clustering

In order to form a plasma that can do measurable damage to an iris tip, a macroscopic area of the surface must be melted in a time that is short compared to the rf pulse length.

A plasma spot formed at the site of a single emitter injects 5 or 10A of electrons into the vacuum above the spot. A significant fraction of these electrons pick up energies up to several hundred keV from the cavity electric fields and then return to bombard the surface in the neighborhood of the spot.

These impacting electrons heat the surface, but not nearly enough to melt it in a time that is short compared to the rf pulse length. In order to melt a large area of the surface, many closely packed plasma spots with overlapping back-bombardment areas, all emitting at the same time, are needed. That is, a crater cluster is required.

The fundamental principle underlying the formation of a crater cluster is that craters attract other craters because of the sharp field emission features formed on a crater rim. Crater clustering is illustrated by the SEM images (next page) of the iris tip region of a traveling-wave structure that has been processed to the breakdown limit.

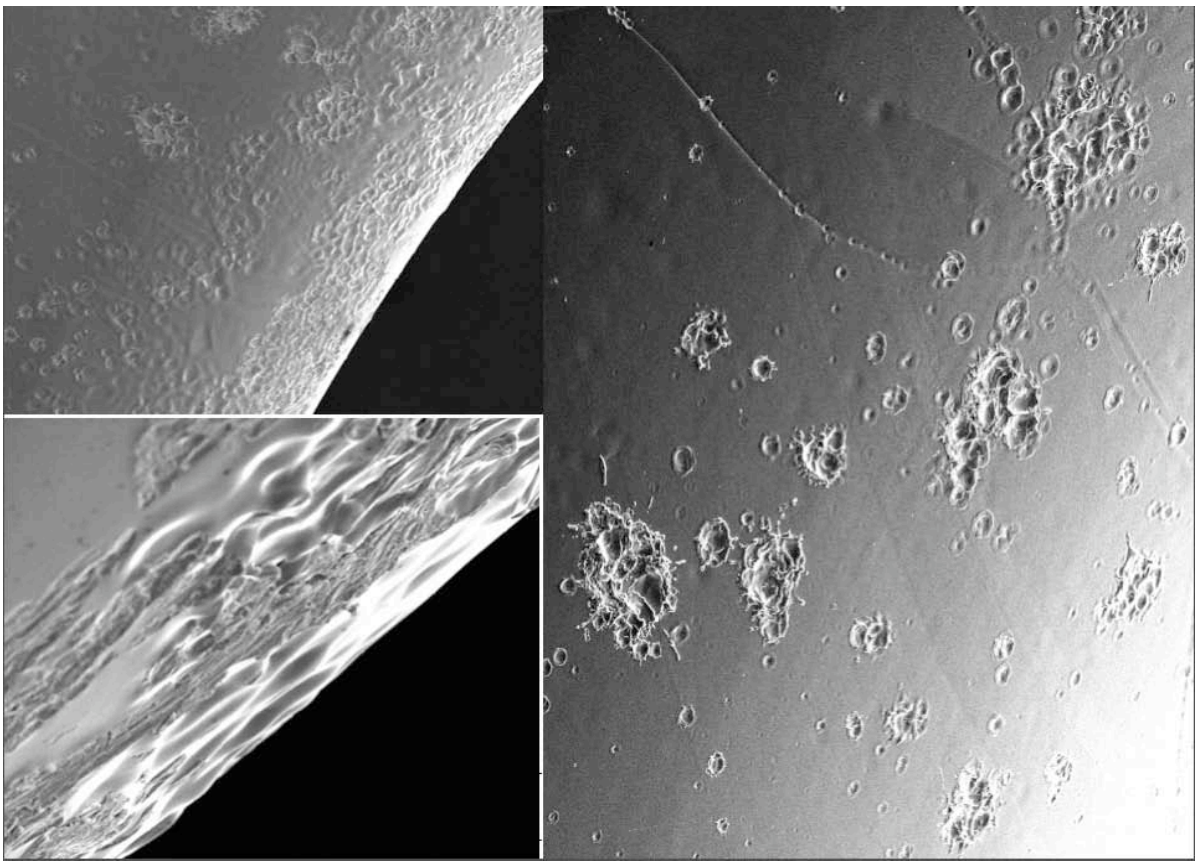

SEM images of an iris tip region in a traveling-wave accelerating structure after processing at the breakdown limit. In the inset at the upper left, individual craters are seen far from the iris tip. Crater clusters grow more numerous as the iris tip is approached. Finally, evidence of surface melting is seen near the tip (images courtesy of Chris Adolphsen, SLAC).

\

Surface Melting

The electric field on a metal surface that is required to melt it in a fixed time, assuming also a fixed electron power incident per unit area from the back-bombarding electrons, depends on the reflective properties of the metal surface and on the bulk properties of the material. These are: the melting temperature, the thermal conductivity, the specific heat, the heat of fusion, the density, and the penetration depth of the electrons. It is assumed that breakdown occurs when a sufficiently large surface area becomes molten. The breakdown fields for various materials, normalized to copper, are shown on the next page. Among the metals beryllium stands out, having a breakdown field about twice that of copper. However, beryllium is not an easy metal to work with. Chromium (normalized breakdown field of about 1.35) and vanadium (normalized breakdown field of about 1.4) are easy to work with and have relatively good breakdown fields. Carbon (improvement factor of about 3.5) is a wild card. There are several ways to make an iris tip out of carbon.

Caution: The enhancement factors in breakdown field for different materials are shown at their ultimate breakdown fields. This is the point at which further processing no longer increases the breakdown field but only damages the structure further. This ranking says nothing about the difficulty of processing when one is well below the ultimate field. This will depend on different material properties and also on the model used to calculate breakdown for individual emitters.

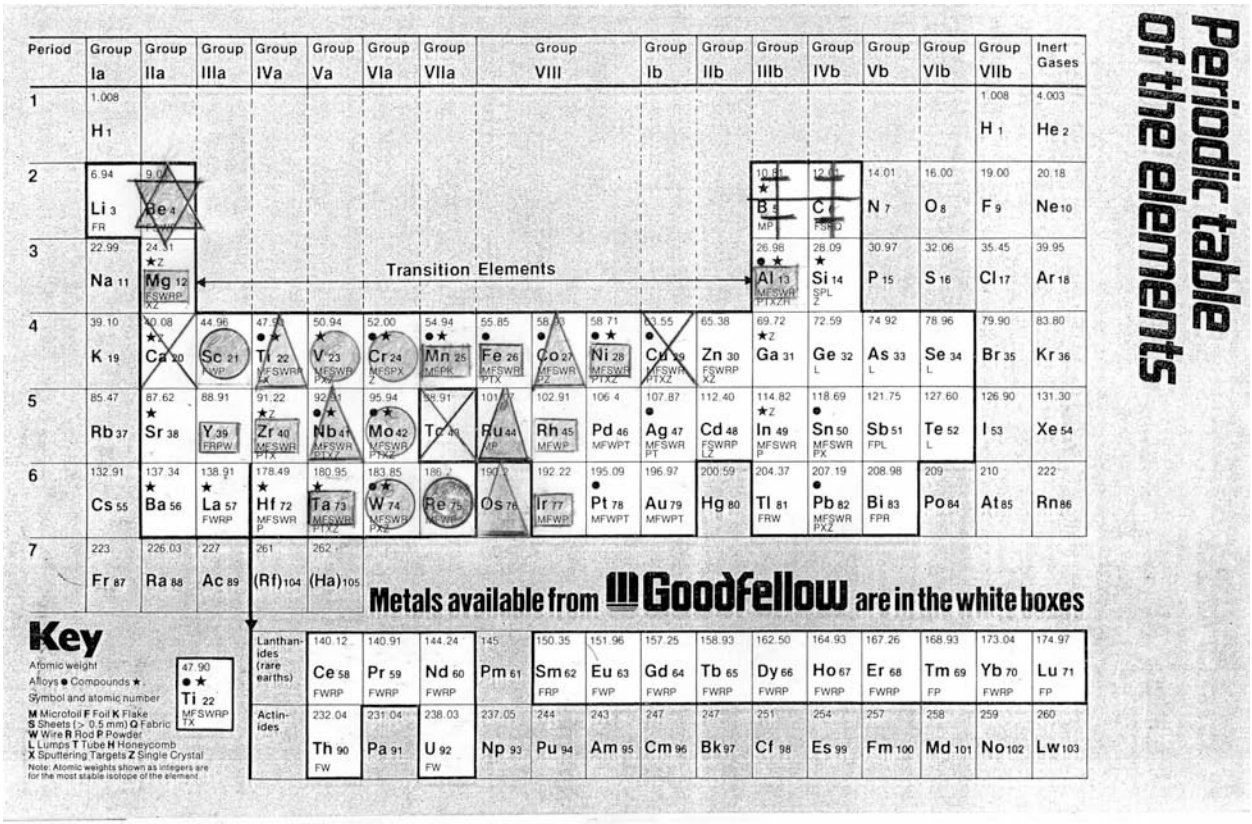

Breakdown Fields Normalized to Copper for Various Metals

< 1.00	1.00 – 1.09	1.10–1.19	1.20–1.29	1.30–1.39	> 1.4
Zn 0.64	Cu 1.00	Zr 1.10	SS 1.20	Re 1.30	Be 2.0
Au 0.80	Ca 1.03	Mn 1.11	Co 1.22	Sc 1.31	
Ag 0.83	Tc 1.07	Y 1.13	Os 1.26	Mo 1.34	*Non-metals*
Pt 0.89		Rh 1.13	Nb 1.27	Cr 1.36	
Hf 0.96		Ta 1.14	Ru 1.27	W 1.37	Si 1.2
Pd 0.97		Al 1.14	Ti 1.29	V 1.39	B 2.3
		Mg 1.15			C 3.7
		Ir 1.17			
		Fe 1.18			
		Ni 1.19			

Taylor Cones

1. A personal observation

The image below shows the formation of structures pulled up by a strong dc electric field acting on the surface of a molten metal [see G. A. Mesyats, *Explosive Electron Emission*, URO-Press, Ekaterinberg, (1998); p.29]. Note the curious shapes of these structures. There are many cone-like objects with a base angle of about 45 degrees. Coming out of the tops of these cones are some roughly cylindrical features having about the same diameter. Some challenges: (1) predict the base angle of the cones; (2) predict the radius of these cylindrical features. The similar radii suggests an instability at a given cone apex radius.

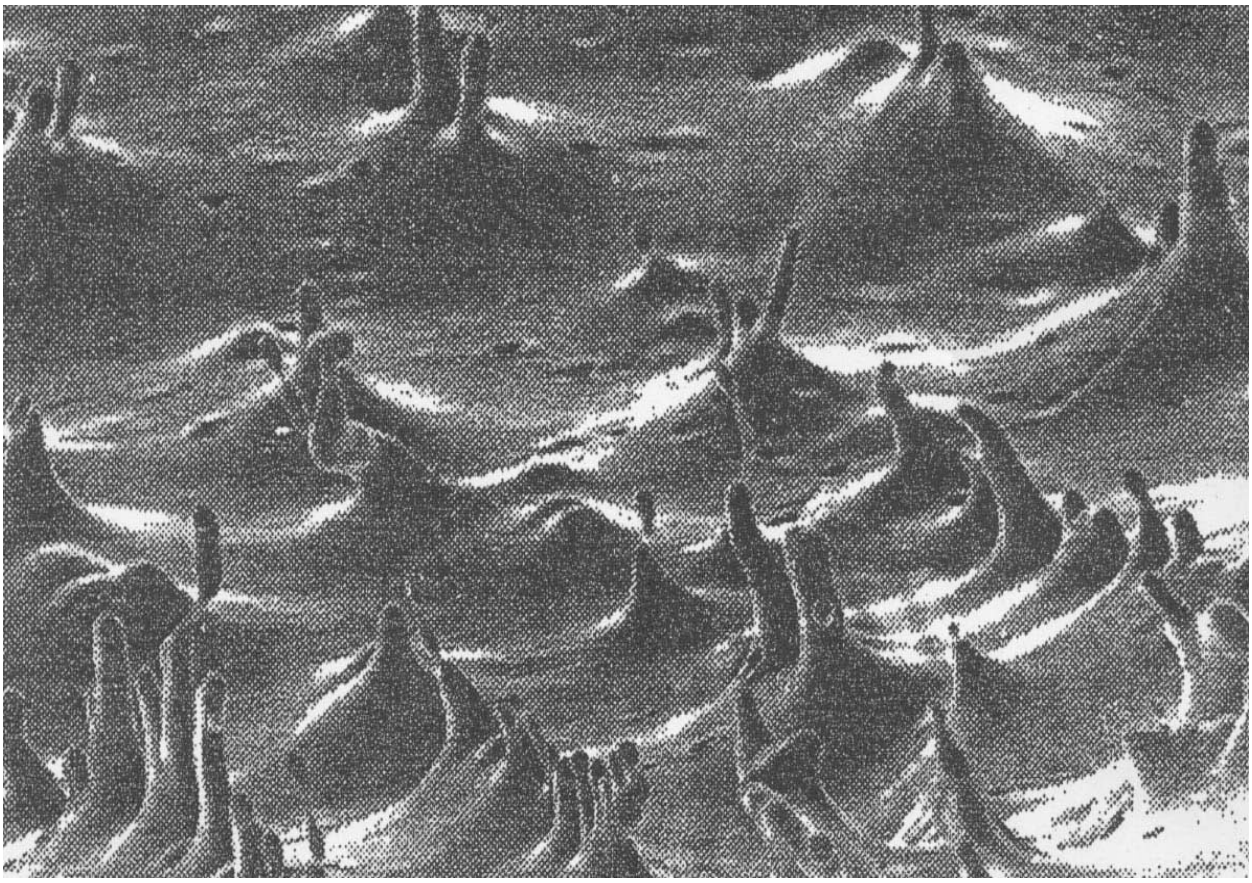

2. The real Taylor

To my knowledge, Geoffrey Taylor was the first person to carefully observe the cone-like objects that form over the surface of a liquid in an intense electric field. In particular, he measured the base angle of the cones and then calculated this angle analytically [Geoffrey Taylor, *Proc. Roy. Soc. A,* **280,** 383 (1964)]. A figure from his paper is shown below.

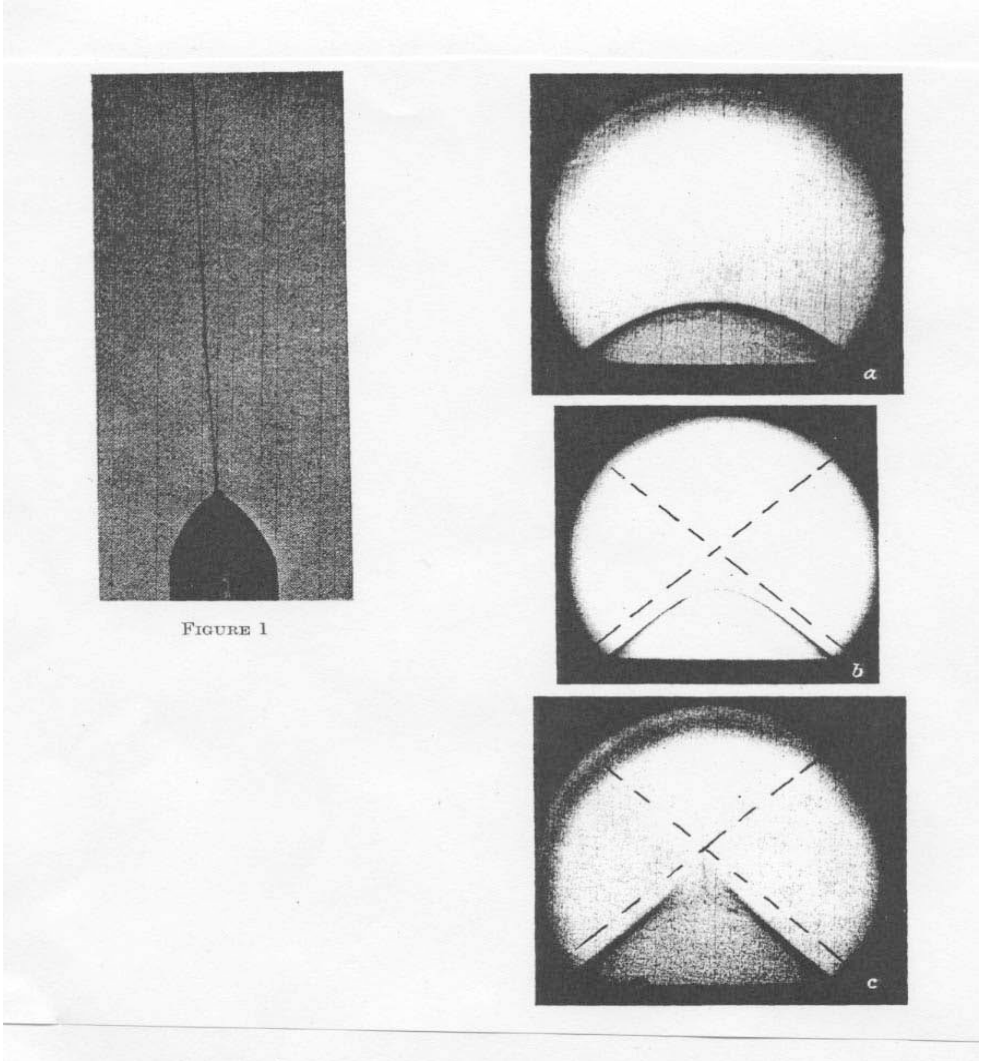

FIGURE 1

Insets *a* through *c* on the right show the effect of an electric field of increasing strength on a water droplet at the tip of a glass capillary tube. In *c* the tip explodes as the radius of the tip approaches a critical value. This occurs at a measured cone apex angle of 98.6°(base angle of 40.7°). In the inset at the left a liquid jet emerges from the tip of a glycerin cone.

The inset in the preceding figure that shows a jet of viscous fluid emerging from the tip of a glycerin Taylor cone also illustrates the principle for forming Kevlar cloth, used for bulletproof vests. A plate covered by a polymer is heated until it becomes a viscous liquid. An electric field is applied and raised until the liquid surface is covered by thousands of Taylor cones. As the field is increased further, polymer jets emerge from the cone tips (like the jet emerging from the tip of a glycerin cone, as shown at the left in the figure on the preceding page). These liquid strings, with diameters in the nanometer range, cross a gap and are deposited in random directions on a cool condensing plate. The material, composed of many layers of these nano-fibers, has incredible mechanical strength.

3. Taylor cones: analytic calculation of the cone base angle

In his paper Taylor first assumes that the cone is conducting. By equating the E^2 force ($\sim r^2E^2$) with the surface tension force ($\sim r$), he finds that E must be proportional to $r^{-1/2}$ along the sides of the cone. He then solves Laplace's equation in cylindrical coordinates, with the cone apex at the origin and the cone extending in the –z direction. Using also the fact that the potential must vanish along the cone sides, the solution to Laplace's equation must have the form $V \sim r^{1/2}P_{1/2}(\cos\theta)$, where $P_{1/2}$ is the Legendre polynomial of order ½ and θ is π minus the cone apex semi-angle. If V is constant along the surface of the cone, then it must be independent of r and $P_{1/2}$ must be zero. This is true for $\theta = 130.7°$ and a half angle of 49.3° for the cone apex.

4. Simulation of the base angle of a Taylor cone

A simulation of the cones shown in the Mesyats figure on page 8, before the instability at the cone tips occurs, is based on the figure below.

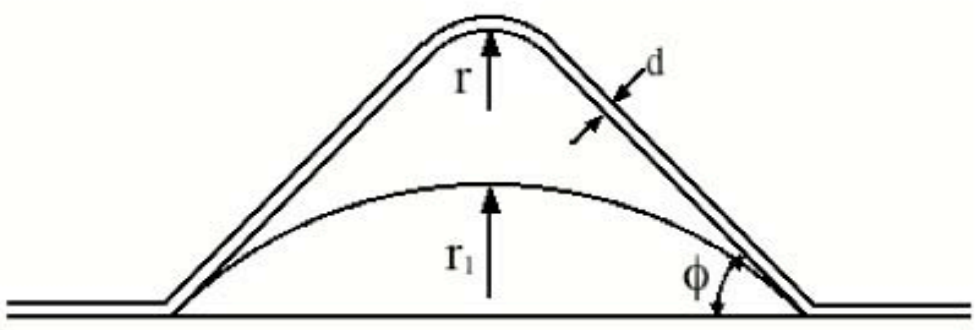

Here ϕ is the base angle of the cone, r is the radius of the cone apex, r_1 is the radius of an initial perturbation, and d is the thickness of a molten layer on the cone surface. This layer is pulled toward the cone tip on each rf pulse, causing the cone to grow (see SLAC–PUB–12354). If the cone tip is a molten liquid in hydrostatic equilibrium, the field enhancement factor β (the ratio of the field at the cone tip to the unperturbed field) must also be proportional to $r^{-1/2}$. This is obtained simply by equating the E^2 pulling force, proportional to E^2r^2, to the force due to surface tension holding the tip in place, which is proportional to r (see also p.3). The result of the simulation is shown on the next page.

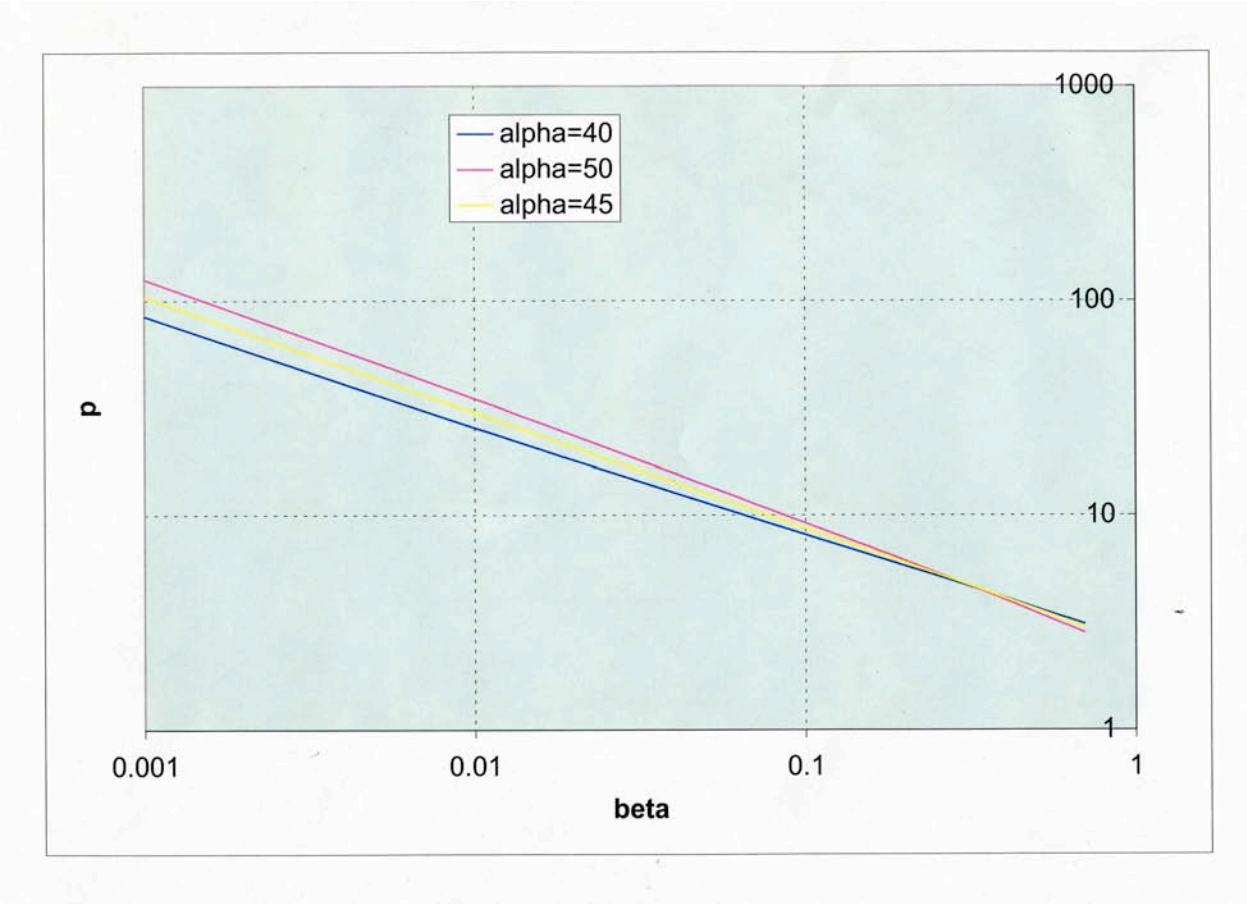

In the figure above (courtesy of Valentin Ivanov) the quantity p, which is proportional to the tip radius r, is plotted as a function of the electric field enhancement factor β for three base angles: 40°, 45° and 50°. The best fit for $\beta \sim r^{-1/2}$ is at a base angle of about 40°, in good agreement with the theoretical value of 40.7°.

Ion Injection

An important application of Taylor cones is to liquid metal ion sources (LMIS) for high performance focused ion beam systems. These beams have probe sizes less than 1μm in diameter. For a more complete discussion see: Jon Orloff, *High-resolution focused ion beams*, Rev. Sci. Instrum. **64**, 1105 (1993). In this article there is also a good review of the physics underlying the formation of Taylor cones, including a calculation of the cone base angle.

Quoting from Orloff's article, "Structurally, an LMIS consists of a liquid metal held in some suitable way to which an electric field strong enough to cause the liquid metal to assume a conical shape has been applied". The end of the cone is drawn to a radius so small that "the high electric field causes ions to begin to form through field evaporation and field ionization of the metal atoms in the vapor". Orloff states that the tip radius of an operating LMIS is on the order of 5 nanometers.

Think of a melted metal surface area, at least 100μm across, in the iris tip region of an accelerating structure. In the presence of a strong electric field hundreds of closely packed Taylor cone will then form (see Mesyats image). As the electric field increases, these cones will begin to act as small ion guns, emitting ions into the high field above the molten surface. This is a recipe, at a critical ion density, for the formation of a plasma with a Debye sheath touching the molten surface. This sheath exerts a pressure of about 1000 Atmospheres on the surface below it. Catastrophic breakdown and macroscopic surface damage follows.